

Observation of conduction electron spin resonance in boron-doped diamondPéter Szirmai,^{1,2} Gábor Fábrián,^{2,*} János Koltai,³ Bálint Náfrádi,¹ László Forró,¹ Thomas Pichler,⁴ Oliver A. Williams,⁵ Soumen Mandal,⁶ Christopher Bäuerle,⁶ and Ferenc Simon^{2,7,†}¹Laboratory of Physics of Complex Matter, École Polytechnique Fédérale de Lausanne, CH-1015 Lausanne, Switzerland²Department of Physics, Budapest University of Technology and Economics, P.O. Box 91, H-1521 Budapest, Hungary³Department of Biological Physics, Eötvös University, Pázmány Péter sétány 1/A, H-1117 Budapest, Hungary⁴Faculty of Physics, University of Vienna, Strudlhofgasse 4, A-1090 Vienna, Austria⁵School of Physics and Astronomy, Cardiff University, Cardiff CF24 3AA, United Kingdom⁶Institut Néel-CNRS and Université Joseph Fourier, 38042 Grenoble, France⁷Condensed Matter Physics Research Group of the Hungarian Academy of Sciences, P.O. Box 91, H-1521 Budapest, Hungary

(Received 4 June 2012; published 28 May 2013)

We observe the electron spin resonance of conduction electrons in boron-doped (6400 ppm) superconducting diamond ($T_c = 3.8$ K). We clearly identify the benchmarks of conduction electron spin resonance (CESR): the nearly temperature independent electron spin resonance signal intensity and its magnitude, which is in good agreement with that expected from the density of states through the Pauli spin susceptibility. The temperature dependent CESR linewidth weakly increases with increasing temperature, which can be understood in the framework of the Elliott-Yafet theory of spin relaxation. An anomalous and yet unexplained relation is observed between the g -factor, CESR linewidth, and the resistivity using the empirical Elliott-Yafet relation.

DOI: [10.1103/PhysRevB.87.195132](https://doi.org/10.1103/PhysRevB.87.195132)

PACS number(s): 76.30.Pk, 71.70.Ej, 75.76.+j

I. INTRODUCTION

Information storage and processing using electron spins, referred to as spintronics,^{1,2} is an ambitious proposition to provide a technological leap in information sciences. The spin-relaxation time in metals and semiconductors, τ_s , is the central parameter which characterizes their utility for spintronic applications.¹ There are two viable routes to determine τ_s in these materials: transport and spectroscopy based. Transport studies usually detect the decay length of an injected nonequilibrium magnetization of a spin ensemble in a nonlocal resistivity measurement.^{3–5} The characteristic decay or spin-diffusion length δ_{spin} contains τ_s through $\delta_{\text{spin}} = v_F \sqrt{\tau \tau_s / d}$, where d is the dimensionality of the material, v_F is the Fermi velocity, and τ is the momentum scattering time. Electron spin resonance (ESR) experiments in metals or semiconductors⁶ are also capable of determining τ_s from the homogeneous ESR linewidth ΔB through $\tau_s = 1/\gamma \Delta B$, where $\gamma/2\pi = 28.0$ GHz/T is the electron gyromagnetic ratio. A spectroscopy related but transport based method is the so-called Hanle spin-precession experiment which also yields τ_s values.¹

In metals with inversion symmetry the so-called Elliott-Yafet theory describes the spin-relaxation properties. It predicts that the spin-relaxation time is proportional to the momentum relaxation time ($\tau_s \propto \tau$) and thus the ESR linewidth is proportional to the resistivity ($\Delta B \propto \rho$).

Heavily boron-doped diamond (BDD) is an example of Mott's metal⁷ above the threshold boron concentration of $n_c \approx 4\text{--}5 \times 10^{20} \text{ cm}^{-3}$.^{8–10} The discovery of superconductivity in BDD (Ref. 11) attracted significant interest and it has been proven that superconductivity in BDD is an intrinsic property which arises from the lightly hole doped diamond bands and not due to the acceptor bands/levels.¹²

Diamond possesses a number of unique properties (such as, e.g., the well-known hardness, large tensile strength, and thermal conductivity) which may lead to a unique class of

fully diamond based integrated (or even spintronic) devices.¹³ Clearly, knowledge of the spin-relaxation time in this new metal is a prerequisite for such applications. In addition, theory of spin relaxation in metals and semiconductors is an ever developing field which progresses by testing the basic theories against new materials.

Herein, we study the electron spin resonance in superconducting BDD ($T_c = 3.8$ K) in the 5–300 K temperature range, i.e., in the normal state. We observe three ESR signals with a temperature dependence which is characteristic for localized paramagnetic centers. In addition, an ESR signal, which is assigned to conduction electrons, is observed. The identification is made by examining the signal intensity and its temperature dependence, which cannot be explained by localized spins. The calibrated signal intensity yields the Pauli spin susceptibility whose experimental value agrees with that obtained from the band-structure-based density of states data. The conduction electron spin resonance (CESR) linewidth increases with increasing temperature which is characteristic for the Elliott-Yafet spin-relaxation mechanism.^{14,15} Measurement of the g -factor and the linewidth allows one to place BDD on the empirical Beuneu-Monod plot,¹⁶ which summarizes the spin-relaxation properties of elemental metals.

II. EXPERIMENT

We performed the ESR experiments on powders of silicon-wafer-free boron-doped diamond samples. To prepare the samples, silicon (111) wafers were cleaned by standard RCA SC1 processes. Diamond nucleation was initiated by immersion of clean wafers in aqueous colloids of hydrogenated nanodiamond particles in an ultrasonic bath. This process is known to produce nucleation densities in excess of 10^{11} cm^{-2} .¹⁷ Diamond growth for 20 h using microwave plasma enhanced chemical vapor deposition with 4% CH_4 diluted in H_2 with 6400 ppm of trimethylboron,¹⁸ microwave

power of 3 kW, and substrate temperature of 800 °C yields films of $\sim 6 \mu\text{m}$ thickness.

Characterization by transport experiments on BDD films found a $T_c = 3.8 \text{ K}$.¹⁹ $T_c \approx 4 \text{ K}$ usually corresponds to a boron concentration of $n \approx 10^{21} \text{ cm}^{-3}$ (or $\sim 6000 \text{ ppm}$) according to the calibration established for samples prepared with chemical vapor deposition.^{20,21} The Si substrate was removed using a mixture of HF and H_2SO_4 . The former oxidizes Si, the latter removes SiO_2 .

Experiments at 9 GHz (0.33 T) were carried out on finely ground BDD samples using a Bruker Elexsys E500 ESR spectrometer in the 5–300 K temperature range. Care was taken to employ large magnetic modulation to enhance the broad resonance signal due to the itinerant electrons and also to eliminate any spurious background signals from the cavity or the cryostat. We used Mn:MgO with a known (1.5 ppm) Mn^{2+} concentration as a g -factor and intensity standard and we also compared the spin susceptibility χ_s against KC_{60} which has a known $\chi_s = 8 \times 10^{-4} \text{ emu/mol}$.²² The ESR spectra are deconvoluted into a sum of derivative Lorentzian curves, which are an admixture of dispersion and absorption lineshapes.

III. RESULTS AND DISCUSSION

The identification of an ESR signal originating from the itinerant electrons in a metal relies on the following benchmarks²³ in the order of importance: (i) the value of the measured spin susceptibility should match the Pauli spin susceptibility, which is related to the density of states (DOS); (ii) the temperature dependence of the signal intensity should be characteristically different from the Curie, i.e., $1/T$, dependence; (iii) for a metal with inversion symmetry, the linewidth should increase with increasing temperature, which is the so-called Elliott-Yafet relaxation mechanism;^{14,15} and (iv) the g -factor shift $\Delta g = g - g_0$ and the ESR linewidth should obey the so-called Elliott-Yafet relation.^{14,15}

Figure 1 illustrates the evolution of the ESR spectrum of BDD from 100 to 300 K. A narrow line with resonance field $B_0 \approx 335 \text{ mT}$ decreases with increasing temperature, whereas

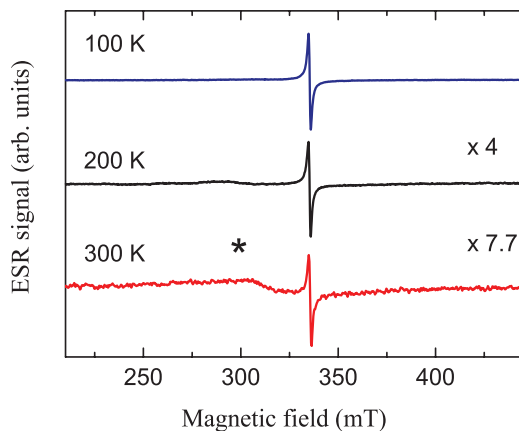


FIG. 1. (Color online) ESR spectra of BDD at different temperatures. Note the broad ESR line (denoted by the asterisk) which is assigned to the conduction electrons. The sharp ESR line originates from localized defect spins.

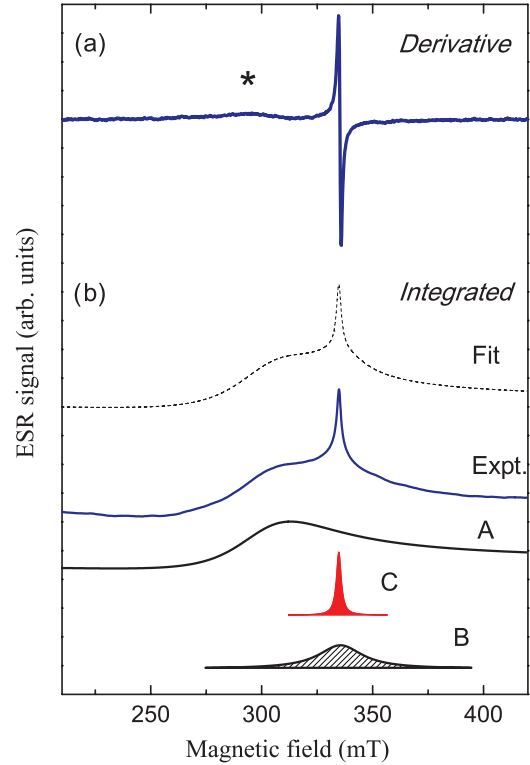


FIG. 2. (Color online) ESR spectrum of BDD at 175 K: (a) raw, derivative data; (b) integrated ESR signal. A fit (Fit) with three components (A, B, and C) simulates well the experiment (Expt.). Note the two narrow signals (B and C), which originate from defects and the broader component (A) coming from the conduction electrons, which displays a Dysonian (asymmetric) lineshape.

the intensity of the broader line with $B_0 \approx 310 \text{ mT}$ does not change significantly.

In Fig. 2(a), we show the ESR spectrum of BDD at 175 K in more detail. In Fig. 2(b), the integrated spectrum is deconvoluted into three curves. In the following, we refer to these as A [$g_A = 2.16(3)$], B [$g_B = 2.003(1)$], and C [$g_C = 2.003(1)$]. The B and C signals are assigned to bulk defects probably accompanying hydrogen vacancy complexes.^{24,25}

The A signal dominates the integrated spectrum at 175 K due to its large linewidth. It is known that broader lines are suppressed compared to the narrower ones in the ESR technique (which uses derivative signals) as the signal amplitude drops with $1/(\Delta B)^2$. Thus the integration visually enhances the broader components.²⁶ The signal A is a strongly asymmetric Lorentzian (known as Dysonian), with an equal mixture of dispersion and absorption components. This ESR lineshape is encountered in metals²⁷ when the itinerant electrons relax their spin state while diffusing through the penetration depth.¹⁹ The other, impurity-related signals do not show a pronounced asymmetry except at lower temperatures (below 35 K), which suggests that the corresponding spins are concentrated close to the grain surfaces.

Below 75 K, we identify a further ESR signal (signal D) with a $g_D = 2.016(1)$ g -factor.¹⁹ Its origin is discussed below. Deconvolution of the ESR spectra into several components varies in the different temperature ranges. The D signal can be followed up to 75 K, however, starting from 75 K the fit

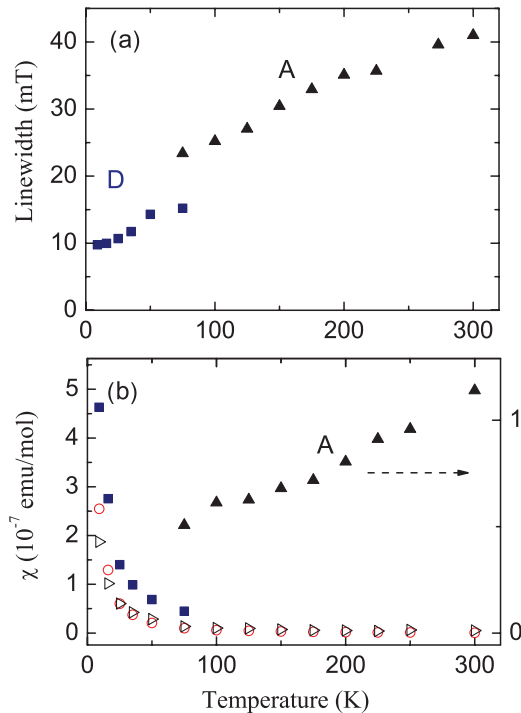


FIG. 3. (Color online) (a) ESR linewidth of the *A* and *D* ESR lines as a function of temperature. (b) Spin susceptibility as obtained from the ESR signal intensity (*A*, \blacktriangle ; *B*, \triangleright ; *C*, \circ ; and *D*, \blacksquare) as a function of temperature. The result for *A* is magnified for better visibility.

converges to the signal *A*. At 75 K the two signals can be fitted independently. Figure 3(a) depicts the ESR linewidth of both *A* and *D* signals as a function of temperature. The linewidth of *A* is 10 mT larger than that of *D* at $T = 75$ K. Hence, we find that the *A* and *D* signals have different origins. Below 75 K the *A* signal cannot be resolved, whose origin is unexplained. We speculate that this effect is caused by weak localization (WL), which may either lead to a sudden line broadening or a loss of spin susceptibility. It is known that WL becomes significant in BDD below around 100–150 K,⁸ which supports that the change of the ESR signal of itinerant electrons and WL may be related. The linewidth of the *A* signal weakly increases with temperature and it has a sizable residual value. These observations are in agreement with the Elliott-Yafet theory of spin relaxation. In addition, the Δg is positive for BDD, which is compatible with the hole nature of charge carriers in BDD.

In Fig. 3(b), the spin susceptibility of the four ESR signals are shown. *B*, *C*, and *D* exhibit a Curie ($\chi_s \propto T^{-1}$) temperature dependence which is characteristic for localized, paramagnetic centers. Their total spin concentration corresponds to ~ 2.2 ppm per carbon atom in our sample;¹⁹ their presence is therefore not expected to substantially modify the intrinsic properties of BDD similar to the hydrogen vacancy complex.²⁸ The ESR intensity of *A* increases by a factor of 2 in the temperature range of 75–300 K. This increase rules out that this signal would originate from localized spins. Instead, its most probable origin is the itinerant conduction electrons in BDD. A similar increase of the CESR signal intensity with a factor of 2–3 was observed in granular MgB_2 samples in the 40–300 K temperature range.^{29,30} Therein, this effect was explained by the limited microwave penetration in the metallic

grains: On increasing temperature the microwave penetration depth increases due to the increasing resistivity, thus resulting in an increasing CESR signal.

Given this slight uncertainty due to the limited microwave penetration, we regard the room temperature CESR signal intensity and associate it with the Pauli spin susceptibility of the itinerant electrons. Calibration of the *A* signal intensity yields $D(E_F) = 4(1) \times 10^{-3}$ states/(eV C-atom) for the density of states of BDD. This value corresponds to a Pauli susceptibility $\chi_s(\text{Pauli}) = \frac{g^2}{4} \mu_B^2 D(E_F) N_A$ of $1.3(3) \times 10^{-7}$ emu/mol = $1.1(3) \times 10^{-8}$ emu/g (here N_A is the Avogadro number and μ_B is the Bohr magneton).

This value is about two orders of magnitude lower spin susceptibility as compared to other metallic carbon phases such as, e.g., K_3C_{60} ($\chi_s \approx 10^{-6}$ emu/g, Ref. 31) or the KC_8 alkali-metal intercalated graphite $\chi_s \approx 6.4 \times 10^{-7}$ emu/g (Ref. 32) due to the small carrier density.

As mentioned above, whether the absolute magnitude of the Pauli spin susceptibility and the corresponding DOS matches the theoretical estimates and other experimental results is an important benchmark to identify a CESR signal. We compare the DOS determined herein with angle-resolved photoemission spectroscopy (ARPES) based DOS data and with theoretical estimates in Fermi-gas- and first-principles-based models. The present DOS value and those based on the ARPES studies are shown in Fig. 4 as a function of T_c . The ARPES-based DOS data are obtained directly from the measured band structure. A free-carrier concentration of $n = 1.1 \times 10^{21} \text{ cm}^{-3}$ which corresponds to 6400 ppm boron doping^{10,19} was used for the Fermi-gas- and first-principles-based DOS calculations, which gave $D(E_F) = 2.4 \times 10^{-2}$ and $D(E_F) = 4 \times 10^{-2}$ in units of states/(eV C-atom), respectively.¹⁹

Clearly, the ARPES-based DOS is in good agreement with the present data, whereas the theoretical estimates significantly differ. We note that the effective carrier concentration in BDD is lowered by the presence of boron dimers,³⁶ which may explain this difference. The presence of boron dimers justifies the use of the truly empirical DOS versus T_c comparison.

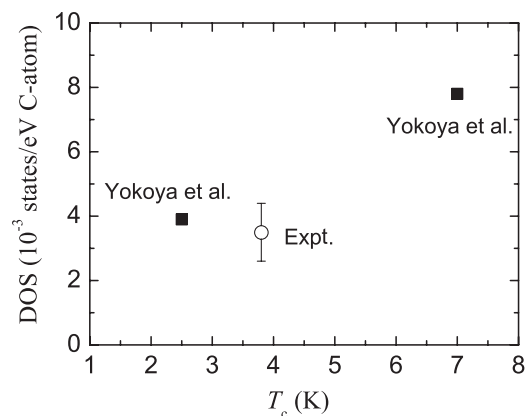


FIG. 4. Density of electronic states in BDD versus T_c . Experimental DOS of the present work (\circ) is shown together with DOS calculated from the ARPES measurements in Ref. 12 (\blacksquare). The error bar in our experiment is a conservative estimate and considers the uncertainty due to the limited microwave penetration depth.

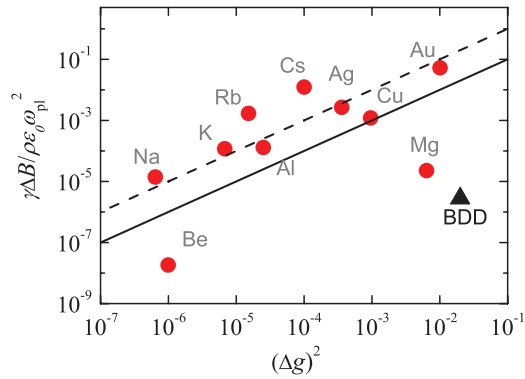


FIG. 5. (Color online) $\gamma \Delta B / \rho \epsilon_0 \omega_{pl}^2$ as a function of Δg^2 [corrected Beuneu-Monod plot (Ref. 33)] for elemental metals (Ref. 16) (●) and BDD (▲). The resistivity data for BDD is taken from Ref. 34. Solid and dashed lines correspond to $\alpha = 1$ and 10, respectively. We use a plasma frequency of $\omega_{pl} = 0.8$ eV after Ref. 35.

In the following, we discuss the validity of the Elliott-Yafet relation $\gamma \Delta B = \alpha (\Delta g)^2 \rho \epsilon_0 \omega_{pl}^2$ (ρ is the resistivity, ϵ_0 is the vacuum permittivity, and ω_{pl} is the plasma frequency) in BDD. The Elliott-Yafet relation combines three independent empirical parameters ΔB , Δg , and ρ , i.e., it is a benchmark of spin-relaxation experiments in novel metals.¹ Beuneu and Monod^{16,37} verified its validity for elemental metals and established a linear scaling, i.e., the empirical constant being $\alpha \approx 1 \dots 10$. In Fig. 5, we show the Beuneu-Monod plot together with the present results for BDD. Clearly, BDD lies out of the general trend observed for most metals. We note that an overestimate of the resistivity may contribute to this effect as the granularity of BDD samples hinders measurement of the intrinsic ρ .³⁸

It is known that the linear scaling of the Elliott-Yafet relation occurs mostly for monovalent materials, and notable exceptions are Be and Mg for which the so-called “hot-spot”

model was invoked to explain the data.³⁹ The hot-spot model recognizes that spin relaxation is enhanced for particular points of the Fermi surface; given that the spin lifetime is much larger than the momentum lifetime, an electron wanders over large portions of the Fermi surface before spin relaxation occurs, i.e., the hot spots dominate the spin relaxation. This effect is pronounced for metals where the Fermi surface strongly deviates from a sphere. We speculate that the deviation observed for BDD from the linear scaling is also caused by a similar effect but its verification requires additional theoretical work.

IV. CONCLUSIONS

In summary, we identified the ESR signal of conduction electrons in boron-doped superconducting diamond. The identification is based on the temperature dependence of the ESR signal intensity and its absolute magnitude. We find that the spin-relaxation mechanism in BDD is dominated by the Elliott-Yafet mechanism. However, we observe an anomalous relationship between the g -factor and the spin-relaxation time, which calls for further theoretical studies. The observed spin-relaxation rate is orders of magnitude smaller than the conventional theory predicts, which enhances the application potential of boron-doped diamond for spintronics.

ACKNOWLEDGMENTS

Useful discussions with András Jánossy are acknowledged. This work was supported by ERC Grant No. ERC-259374-Sylo, New Széchenyi Plan No. TÁMOP-4.2.2.B-10/1.2010-0009, and Hungarian State Grants (OTKA) No. K81492. The Swiss NSF is acknowledged for support. S.M. and C.B. acknowledge financial support by the French National Agency (ANR) in the frame of its program in “Nanosciences and Nanotechnologies” (SUPERNEMS project ANR-08-PNANO-033).

*Present address: Department of Physics, University of Basel, Klingelbergstrasse 82, CH-4056 Basel, Switzerland.

†Corresponding author: ferenc.simon@univie.ac.at

¹I. Žutić, J. Fabian, and S. D. Sarma, *Rev. Mod. Phys.* **76**, 323 (2004).

²M. Wu, J. Jiang, and M. Weng, *Phys. Rep.* **493**, 61 (2010).

³N. Tombros, C. Józsa, M. Popinciuc, H. T. Jonkman, and B. J. van Wees, *Nature (London)* **448**, 571 (2007).

⁴T.-Y. Yang, J. Balakrishnan, F. Volmer, A. Aysar, M. Jaiswal, J. Samm, S. R. Ali, A. Pachoud, M. Zeng, M. Popinciuc *et al.*, *Phys. Rev. Lett.* **107**, 047206 (2011).

⁵W. Han and R. K. Kawakami, *Phys. Rev. Lett.* **107**, 047207 (2011).

⁶T. W. Griswold, A. F. Kip, and C. Kittel, *Phys. Rev.* **88**, 951 (1952).

⁷N. Mott, *J. Non-Cryst. Solids* **1**, 1 (1968).

⁸T. Klein, P. Achatz, J. Kacmarcik, C. Marcenat, F. Gustafsson, J. Marcus, E. Bustarret, J. Pernot, F. Omnes, B. E. Sernelius *et al.*, *Phys. Rev. B* **75**, 165313 (2007).

⁹E. Bustarret, P. Achatz, B. Sacépé, C. Chapelier, C. Marcenat, L. Ortéga, and T. Klein, *Philos. Trans. R. Soc. London, Ser. A* **366**, 267 (2008).

¹⁰We refer to the nominal concentration of the boron atoms throughout the text which is higher than the actual carrier concentration due to the tendency of boron dimer formation, which does not contribute to free carriers.

¹¹E. A. Ekimov, V. A. Sidorov, E. D. Bauer, N. N. Mel’nik, N. J. Curro, J. D. Thompson, and S. M. Stishov, *Nature (London)* **428**, 542 (2004).

¹²T. Yokoya, T. Nakamura, T. Matsushita, T. Muro, Y. Takano, M. Nagao, T. Takenouchi, H. Kawarada, and T. Oguchi, *Nature (London)* **438**, 647 (2005).

¹³S. Mandal, T. Bautze, O. A. Williams, C. Naud, E. Bustarret, F. Omnes, P. Rodière, T. Meunier, C. Bäuerle, and L. Saminadayar, *ACS Nano* **5**, 7144 (2011).

¹⁴R. J. Elliott, *Phys. Rev.* **96**, 266 (1954).

¹⁵Y. Yafet, *Phys. Lett. A* **98**, 287 (1983).

¹⁶F. Beuneu and P. Monod, *Phys. Rev. B* **18**, 2422 (1978).

- ¹⁷J. Hees, A. Kriele, and O. A. Williams, *Chem. Phys. Lett.* **509**, 12 (2011).
- ¹⁸W. Gajewski, P. Achatz, O. A. Williams, K. Haenen, E. Bustarret, M. Stutzmann, and J. A. Garrido, *Phys. Rev. B* **79**, 045206 (2009).
- ¹⁹See Supplemental Material at <http://link.aps.org/supplemental/10.1103/PhysRevB.87.195132> for the results of SEM, Raman, and transport measurements, as well as the description of the first-principles calculations.
- ²⁰H. Mukuda, T. Tsuchida, A. Harada, Y. Kitaoka, T. Takenouchi, Y. Takano, M. Nagao, I. Sakaguchi, and H. Kawarada, *Sci. Technol. Adv. Mater.* **7**, S37 (2006).
- ²¹Y. Takano, T. Takenouchi, S. Ishii, S. Ueda, T. Okutsu, I. Sakaguchi, H. Umezawa, H. Kawarada, and M. Tachiki, *Diamond Relat. Mater.* **16**, 911 (2007).
- ²²G. Oszlányi, G. Bortel, G. Faigel, M. Tegze, L. Gránásy, S. Pekker, P. W. Stephens, G. Bendele, R. Dinnebier, G. Mihály *et al.*, *Phys. Rev. B* **51**, 12228 (1995).
- ²³P. Szirmai, G. Fábíán, B. Dóra, J. Koltai, V. Zólyomi, J. Kürti, N. M. Nemes, L. Forró, and F. Simon, *Phys. Status Solidi B* **248**, 2688 (2011).
- ²⁴X. Zhou, G. D. Watkins, K. M. McNamara Rutledge, R. P. Messmer, and S. Chawla, *Phys. Rev. B* **54**, 7881 (1996).
- ²⁵N. Mizuochi, H. Watanabe, H. Okushi, S. Yamasaki, J. Niitsuma, and T. Sekiguchi, *Appl. Phys. Lett.* **88**, 091912 (2006).
- ²⁶A. Jánossy, O. Chauvet, S. Pekker, J. R. Cooper, and L. Forró, *Phys. Rev. Lett.* **71**, 1091 (1993).
- ²⁷G. Feher and A. F. Kip, *Phys. Rev.* **98**, 337 (1955).
- ²⁸N. Mizuochi, M. Ogura, H. Watanabe, J. Isoya, H. Okushi, and S. Yamasaki, *Diamond Relat. Mater.* **13**, 2096 (2004).
- ²⁹F. Simon, A. Jánossy, T. Fehér, F. Murányi, S. Garaj, L. Forró, C. Petrovic, S. L. Bud'ko, G. Lapertot, V. G. Kogan *et al.*, *Phys. Rev. Lett.* **87**, 047002 (2001).
- ³⁰F. Simon, A. Jánossy, T. Fehér, F. Murányi, S. Garaj, L. Forró, C. Petrovic, S. Bud'ko, R. A. Ribeiro, and P. C. Canfield, *Phys. Rev. B* **72**, 012511 (2005).
- ³¹O. Gunnarsson, *Rev. Mod. Phys.* **69**, 575 (1997).
- ³²M. S. Dresselhaus and G. Dresselhaus, *Adv. Phys.* **51**, 1 (2002).
- ³³G. Fábíán, B. Dóra, A. Antal, L. Szolnoki, L. Korecz, A. Rockenbauer, N. M. Nemes, L. Forró, and F. Simon, *Phys. Rev. B* **85**, 235405 (2012).
- ³⁴J. Mareš, P. Hubík, M. Nesládek, D. Kindl, and J. Krištofik, *Diamond Relat. Mater.* **15**, 1863 (2006).
- ³⁵M. Ortolani, S. Lupi, L. Baldassarre, U. Schade, P. Calvani, Y. Takano, M. Nagao, T. Takenouchi, and H. Kawarada, *Phys. Rev. Lett.* **97**, 097002 (2006).
- ³⁶E. Bourgeois, E. Bustarret, P. Achatz, F. Omnès, and X. Blase, *Phys. Rev. B* **74**, 094509 (2006).
- ³⁷P. Monod and F. Beuneu, *Phys. Rev. B* **19**, 911 (1979).
- ³⁸G. Zhang, S. D. Janssens, J. Vanacken, M. Timmermans, J. Vacík, G. W. Ataklti, W. Decelle, W. Gillijns, B. Goderis, K. Haenen *et al.*, *Phys. Rev. B* **84**, 214517 (2011).
- ³⁹J. Fabian and S. Das Sarma, *Phys. Rev. Lett.* **81**, 5624 (1998).